Blockade of the erbB2 Receptor Induces Cardiomyocyte Death through Mitochondrial and Reactive Oxygen Species-dependent Pathways*

Leo I. Gordon[‡§], Michael A. Burke[¶], Amareshwar T. K. Singh[‡§], Sheila Prachand[‡§], Elliot D. Lieberman[‡], Lin Sun[¶], Tejaswitha Jairaj Naik[¶], Sathyamangla V. Naga Prasad[‖], and Hossein Ardehali[‡§1]

From the [‡]Division of Hematology/Oncology and the [¶]Division of Cardiology, Department of Medicine, and the [§]Robert H. Lurie Comprehensive Cancer Center, Northwestern University, Chicago, Illinois 60611 and the [‖]Department of Molecular Cardiology, Lerner Research Institute, Cleveland Clinic Foundation, Cleveland, Ohio 44195

Overexpression of the receptor tyrosine kinase erbB2 (Her2 in humans) is correlated with a poor prognosis in breast and ovarian cancers. Treatment with trastuzumab (a monoclonal antibody against erbB2) improves survival; however, it also causes cardiomyopathy. We hypothesized that blockade of the erbB2 receptor induces cardiomyocyte death through a mitochondrial pathway that is dependent on the production of reactive oxygen species (ROS). We first showed that levels of erbB2 receptor are significantly decreased in an animal model of ischemic heart disease and in human ischemic cardiomyopathy. We treated neonatal rat cardiomyocytes with an inhibitory erbB2 antibody to study the mechanism behind the deleterious effects of erbB2 blockade. These cells displayed a dose-dependent increase in ROS production and cell death compared with control IgG-treated cells; these processes were reversed by the antioxidant, N-acetylcysteine. The effects of erbB2 antibody on both cell death and ROS production were also reversed by cyclosporine A and diazoxide, chemicals that regulate the pro- and anti-apoptotic channels in the mitochondria, respectively. Furthermore, mouse embryonic fibroblasts lacking Bax and Bak (proteins that mediate cell death through a mitochondrial pathway) were resistant to the deleterious effects of erbB2 antibody. These effects of erbB2 blockade appear to occur through a pathway involving AKT and PKC-α. Our results suggest that erbB2 plays a role in cardiomyocyte survival, and that the deleterious effects of trastuzumab on the heart occur through a mitochondrial pathway and is mediated by ROS production. Manipulation of redox signaling may be beneficial in cancer patients receiving trastuzumab.

The Her-2/neu oncogene, also known as erbB2 in nonhuman organisms, is a transmembrane receptor tyrosine kinase that belongs to the epidermal growth factor receptor family (1, 2).

Overexpression of Her2 is seen in ~30% of breast cancer patients and is associated with poor survival, increased metastasis, and resistance to chemotherapy (3–5). Transgenic mice overexpressing erbB2 develop focal mammary tumors, thus implicating this protein in tumorigenesis (6). Trastuzumab (Herceptin, Genentech, CA) is a monoclonal antibody (Ab)[2] that binds to Her2 with high affinity and improves survival of patients with advanced breast cancer (7). Trastuzumab is clinically efficacious both as a single agent or in combination with standard chemotherapy regimens (4–6). However, this agent is cardiotoxic on its own, and especially when administered with anthracyclines, where it can cause cardiomyopathy (CM) in up to 27% of patients (8).

The importance of erbB2 in normal cardiac development and physiology was demonstrated in mice by cardiac-specific knock-out of erbB2 (9, 10). The mice were initially normal, but developed CM as adults. One study demonstrated no difference between the wild-type and knock-out mice in the degree of cardiac cell death as assessed by TUNEL staining (10). However, in another study that used a more sensitive PCR-based DNA fragmentation assay increased DNA fragmentation was reported in the hearts of erbB2-knock-out animals (9). Recently, Grazette et al. (11) studied the effects of erbB2 blockade on cardiomyocyte survival, and showed that erbB2 antibody (erbB2-Ab) caused a loss of mitochondrial membrane potential and an increase in cell death.

The mechanism for the deleterious effects of erbB2 blockade remains unclear, but a recent report showed that activation of erbB2 reduces doxorubicin-induced oxidative stress in cardiomyocytes (12). Therefore, we hypothesized that erbB2-Ab-induced cell death in cardiomyocytes is a mitochondrial dependent process that involves ROS production. In this report, we show that erbB2 levels are decreased in an animal model of myocardial ischemia and in patients with ischemic CM. We

[2] The abbreviations used are: Ab, antibody; ROS, reactive oxygen species; CM, cardiomyopathy; NAC, N-acetylcysteine; NRCM, neonatal rat cardiomyocytes; TMRE, tetramethylrhodamine ethyl ester; PBS, phosphate-buffered saline; DCF and H_2DCFDA, 5-(and-6)-carboxy-2′,7′-dichlorodihydrofluorescein diacetate; LCx, left circumflex coronary artery; LAD, left anterior descending coronary artery; CsA, cyclosporine A; mPTP, mitochondrial permeability transition pore; mitoK_{ATP}, mitochondrial ATP-sensitive potassium channel; MEF, mouse embryonic fibroblasts; DKO, double knockout; WT, wild type; TUNEL, terminal deoxynucleotidyltransferase-mediated dUTP nick end-labeling.

then demonstrate that erbB2 blockade in cardiomyocytes leads to ROS production, and that the antioxidant *N*-acetylcysteine (NAC) protects against the damage induced by erbB2-Ab. We also find that erbB2 signaling in cardiomyocytes occurs through a mitochondrial, AKT-, and PKCα-dependent pathway. Moreover, the deleterious effects caused by the loss of erbB2 function require the pro-apoptotic proteins Bax and Bak. Finally, by using an erbB2-specific siRNA, we demonstrate that the effects of erbB2 blockade evolve from the specific inhibition of the erbB2 pathway rather than through nonspecific effects of the antibody. Together, our results suggest that erbB2 blockade increases ROS through a mitochondrial pathway.

EXPERIMENTAL PROCEDURES

Human Heart Samples—Non-failing, failing non-ischemic, and ischemic human heart samples were obtained from the Human Heart Tissue Bank at Cleveland Clinic Foundation. The failing non-ischemic and ischemic human heart tissues were procured from the explanted hearts of cardiac transplant recipients. Non-failing samples were obtained from unmatched organ donors with no history of cardiac disease (as measured by echocardiography) whose ejection fractions were >55% and whose hearts were unsuitable for transplantation. The explanted hearts were immediately placed in cold cardioplegic solution and were subsequently frozen in liquid nitrogen for biochemical analysis. Protocols for tissue procurement were approved by the Institutional Review Board of the Cleveland Clinic Foundation. Informed consent was obtained from all transplant patients and from the families of the organ donors before tissue collection.

Frozen samples were homogenized in Nonidet P-40 lysis buffer (1% Nonidet P-40, 10% glycerol, 137 mM NaCl, 20 mM Tris-Cl, pH 7.4, 1 mM phenylmethylsulfonyl fluoride, 20 mM NaF, 1 mM sodium pyrophosphate, 1 mM sodium orthovanadate, and 2 μg/ml each of aprotinin and leupeptin) and centrifuged at 37,500 $\times$ *g* for 25 min at 4 °C. The myocardial extract (120 μg) was resolved on a 10% SDS-PAGE gel, and Western blotting was subsequently performed as described below.

Ischemic Dog Tissue Extracts—Dog tissue samples were kindly provided by Dr. Robert Decker (Northwestern University). Experimental ischemic animal preparation was performed as described previously (13). Tissue samples from dogs undergoing 75% left circumflex coronary artery occlusion were homogenized on ice in radioimmune precipitation assay buffer with the addition of protease inhibitors (Roche Applied Science). Total protein was quantified via Bradford assay, and 40 μg of each sample was subjected to SDS-PAGE followed by Western blotting as described below.

Preparation of Neonatal Rat Cardiomyocytes (NRCM)—NRCM preparation was performed as described previously (14). Cells were treated with control rabbit IgG or erbB2 IgG antibody for 24 h before viability studies or measurement of ROS levels. For Western blotting, mitochondria were isolated by using a kit from Pierce Biotechnology.

Viability Studies—The mitochondrial membrane depolarizes rapidly at the onset of cell death. The mitochondrial membrane potential ($\Delta\Psi_m$) is a marker of cell injury and is assessed by using 100 nM of the fluorescent dye, tetramethylrhodamine

ethyl ester (TMRE). After addition of TMRE, $\Delta\Psi_m$ was measured by flow cytometry. For trypan blue studies, cells were detached and suspended in phosphate-buffered saline (PBS). An equal volume of trypan blue was then added, and the numbers of unstained (viable) and stained (non-viable) cells were counted using a hemocytometer. The proportion of viable cells was determined by calculating the percentage of unstained cells. Three different counts were performed in at least three independent experiments for each group.

Confocal Microscopy—Confocal microscopy was performed with an LSM 510 META laser scanning microscope (Zeiss, Thornwood, NY). The following wavelengths were used for excitation: 488 nm for green, 543 nm for red, and 405 nm for blue. Filters used for emission were: 505–530 nm for green, 565–615 nm for red, and 420–480 nm for blue. The lens objective was 40x Plan-NEOFLUAR NA 1.4 for red mitochondrial superoxide indicator (mitoSOX) and DCF studies. LSM 510 software (Zeiss) was used for data analysis.

RNA Interference Experiments—An siRNA for erbB2 that had been previously used to knockdown erbB2 levels in NRCM was synthesized (Qiagen) (11). Non-silencing siRNA sequences from Qiagen and Dharmacon were used for control experiments. RNA duplexes were transfected into NRCM with a TransMessenger Kit (Qiagen).

ROS Measurements—For studies with 5-(and-6)-carboxy-2′,7′-dichlorodihydrofluorescein diacetate (H$_2$DCFDA), myocytes were harvested by trypsinization, washed with Ca^{2+}- and Mg^{2+}-free PBS, and suspended in 0.5 ml of PBS. H$_2$DCFDA was then added, and cells were incubated at 37 °C in the dark for 30 min. Cells were washed, suspended in PBS, and analyzed by confocal microscopy or flow cytometry with excitation at 488 nm and emission at 530-nm wavelength. For mitoSOX studies, 5 μM mitoSOX was added to NRCM, and cells were analyzed by flow cytometry.

Western Blots—40 μg of dog myocardial extracts, 120 μg of human myocardial extracts, or NRCM mitochondrial extracts were resolved on 10% SDS-PAGE gels (Invitrogen). Proteins were transferred to nitrocellulose membranes (Invitrogen) and Western blotting was performed to detect erbB2 (anti-Neu, C-18) or cytochrome *c* (cyto *c*). Other antibodies used in our experiments are: AKT, phospho-AKT, PKCα and phosphor-PKCα (all purchased from Cell Signaling). Control IgG was purchased from Sigma-Aldrich. The blots were stripped and re-probed with anti-actin (I-19) antibody (human samples), anti-GAPDH antibody (dog samples), or anti-ATPase antibody (NRCM mitochondrial samples), which were used for normalization. All antibodies were obtained from Santa Cruz Biotechnology.

Chemiluminescent images were captured with an Epson Perfection 3490 Photo scanner, and the band intensities were determined with ImageJ analysis software (NIH). Data were quantified as the ratio of the luminescence of the given protein to that of the internal control.

Statistical Analysis—Data are expressed as mean $\pm$ S.E. Unpaired Student's *t* tests were performed for statistical comparisons. For all tests, a *p* value of less than 0.05 was considered significant.
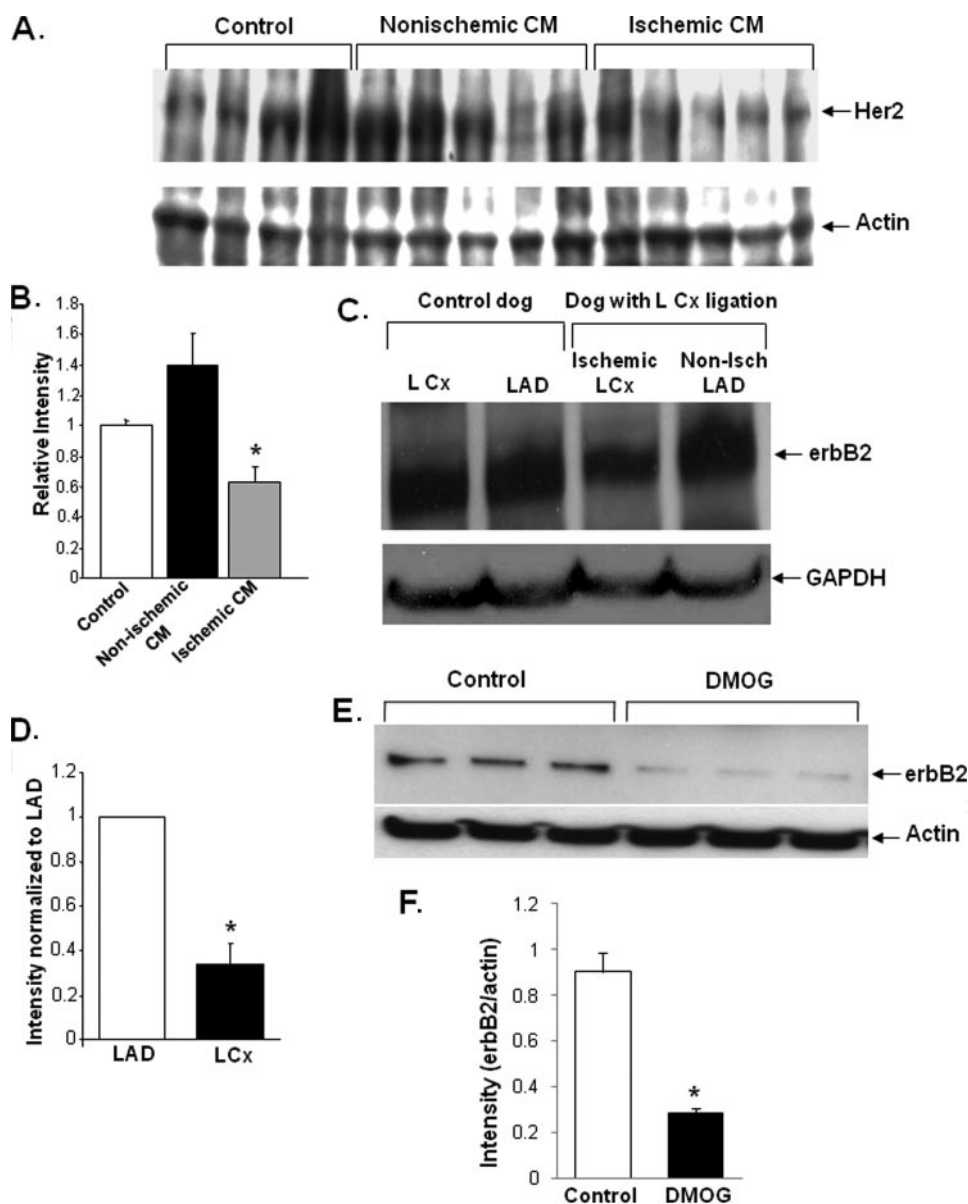
FIGURE 1. **Ischemia decreases the level of erbB2 protein in cardiomyocytes.** *A*, Western blot with Her2 antibody on samples from normal human hearts (control) and from the hearts of patients with non-ischemic cardiomyopathy or ischemic cardiomyopathy. Four normal samples and five samples from ischemic and nonischemic cardiomyopathy patients were included in our studies. *B*, band densitometry was performed on the blot shown in *A*, and Her2 levels were normalized to actin levels (*, $p = 0.011$ *versus* control). *C*, Western blot for erbB2 protein levels in the hearts of dogs subjected to ischemia in the LCx artery for 2–5 h then immediately sacrificed. Tissue samples from the LCx (ischemic) and LAD (non-ischemic) territories were isolated along with similar samples from sham-instrumented (control) animals, which underwent all surgical procedures except coronary artery constriction, $n = 3$ in each group. *D*, quantification of erbB2 levels from Western blots similar to those shown in *C*. (*, $p = 0.009$ *versus* LAD). *E*, Western blot of NRCM treated with DMOG (a HIF-stabilizer) and control NRCM. *F*, quantification of erbB2 levels from the Western blots in *E*. DMOG treatment resulted in a significant decrease in the levels of erbB2 (*, $p < 0.05$ *versus* control). Band intensities were measured using ImageJ and normalized to the internal control (GAPDH or actin). Data are presented as mean ± S.E.

RESULTS

Ischemia Decreases Levels of erbB2 Protein in Cardiomyocytes— To understand the role of the erbB2 pathway in cardiomyocyte survival, we first used Western blots to measure the levels of erbB2 in the explanted hearts of patients with ischemic or non-ischemic CM, as well as in normal hearts from organ donors that were unsuitable for transplant. Compared with normal hearts, the level of erbB2 protein was ~40% lower in hearts from patients with ischemic CM, and a nonstatistically

significant increase in erbB2 levels was observed in patients with non-ischemic CM (Fig. 1, *A* and *B*). These results suggest that erbB2 levels in the heart decline only in response to ischemic damage.

To better assess the role of erbB2 in ischemic injury, dogs were subjected to left circumflex (LCx) coronary constriction, which reduced coronary flow in the LCx territory by 75% (as determined by microsphere blood flow analysis) (13). Extracts of heart tissue from dogs subjected to LCx constriction were examined by Western blotting to determine erbB2 levels. Tissue samples from both LCx (ischemic) and left anterior descending (LAD, nonischemic) territories were included in our studies. ErbB2 levels were reduced ~60% in the ischemic LCx territory compared with the non-ischemic LAD samples (Fig. 1, *C* and *D*). Together with our findings in human CM samples, these results suggest that erbB2 levels are reduced in response to both acute and chronic ischemic damage.

To assess whether the effects of ischemia on erbB2 occur through a pathway that is dependent on hypoxia-inducible factor (HIF), erbB2 levels were measured in NRCM that had been treated with 500 μM of 1 dimethyloxallyl glycine (DMOG), which inhibits *HIF-α* prolyl hydroxylase and stabilizes HIF. As shown in Fig. 1, *E* and *F*, cells treated with DMOG displayed a significant decrease in the levels of erbB2, suggesting that the response to hypoxia occurs through a HIF-dependent pathway.

*Treatment with erbB2-Ab Increases Cell Death and ROS Production—*Recently, it has been demonstrated that activation of the erbB2 receptor by neuregulin-1-reduced doxorubicin-induced oxidative stress in adult rat cardiomyocytes (12), suggesting that the erbB2 pathway has a role in the inhibition of ROS production. We hypothesized that the deleterious effects of erbB2 blockade are caused by an increase in ROS production. To test this hypothesis, we assessed viability and ROS levels in NRCM treated with erbB2-Ab or pre-immune rabbit IgG as a control. Treatment with erbB2-Ab caused a significant and specific increase in cell death, as measured by TMRE uptake and trypan blue exclusion
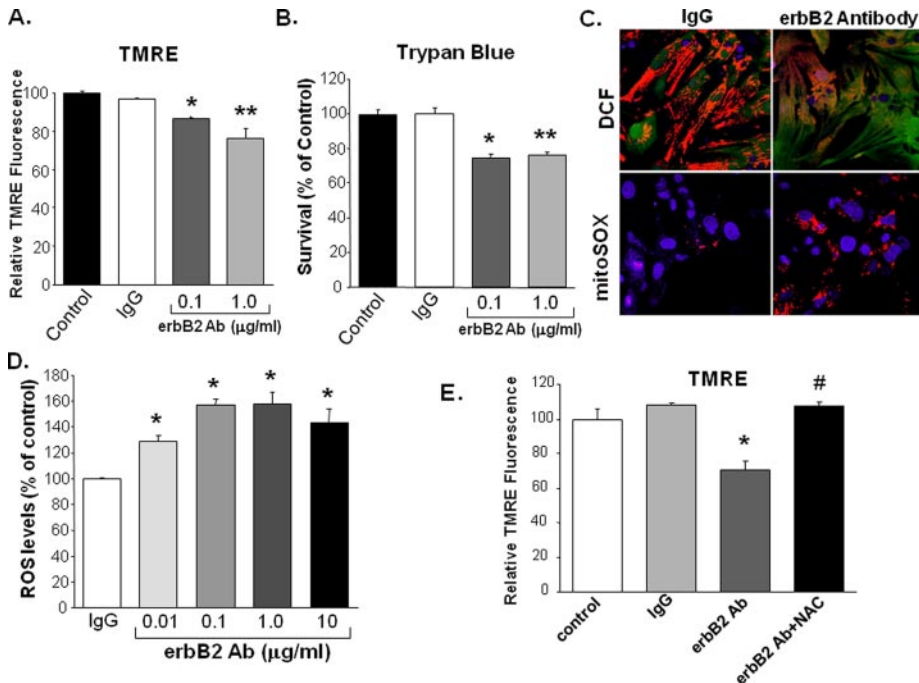
FIGURE 2. **Treatment of NRCM with an erbB2 antibody increases ROS production, and the increase is blocked by treatment with NAC.** NRCM were treated with 0.1 or 1 μg/ml of erbB2 antibody, and cell death was measured via (*A*) TMRE uptake (*, $p = 0.017$ and **, $p = 0.029$ compared with IgG, $n \geq 3$) or (*B*) trypan-blue exclusion studies (*, $p = 0.016$ and **, $p = 0.003$ compared with IgG, $n \geq 3$). *C*, ROS production was assessed by using confocal microscopy to visualize DCF (*top panels*, *green fluorescence*) and mitoSOX (*bottom panels*, *red fluorescence*) markers. The *top panels* were also stained with TMRE to identify mitochondria (*red*) and the *bottom panels* were stained with DAPI to identify nuclei (*blue*). *D*, quantification of ROS production in cells treated with rabbit pre-immune IgG (control) or erbB2 antibody for 18 h. ROS was detected by flow cytometry for DCF, and results were normalized to control cells treated with 1 μg/ml of IgG (*, $p < 0.05$ *versus* IgG; $n \geq 3$). *E*, treatment with 10 mM NAC increases cell survival in the presence of erbB2 Ab. NRCM were treated with erbB2 Ab in the presence and absence of NAC, and viability was measured 24 h later via TMRE uptake (*, $p = 0.007$ *versus* IgG; #, $p = 0.016$ *versus* erbB2 Ab; $n = 3$). Data are presented as mean ± S.E.
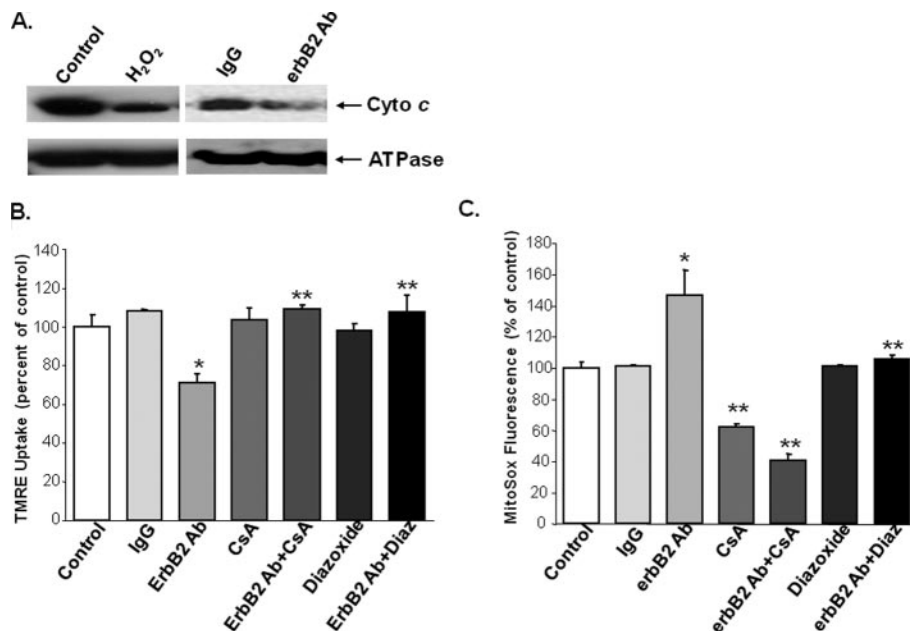

FIGURE 3. **erbB2-mediated signaling occurs through a mitochondria-dependent pathway.** *A*, mitochondrial extracts from untreated (control) NRCM and from NRCM treated with erbB2 Ab were analyzed by Western blot with cyto *c* antibodies. ATP synthase (ATPase), a mitochondrial protein, was used as an internal control. *B*, NRCM were treated with erbB2 Ab in the presence and absence of the mPTP inhibitor CsA or the mitoK$_{ATP}$ activator diazoxide, and viability was assayed via TMRE and flow cytometry. Both CsA and diazoxide reverse the deleterious effects of the erbB2 Ab (*, $p = 0.007$ *versus* IgG and **, $p < 0.05$ *versus* erbB2 Ab; $n \geq 3$). The untreated (control) cells displayed in Fig. 2E were used as controls for this analysis. *C*, quantification of ROS production using the mitoSOX assay. *, $p < 0.05$ *versus* IgG and **, $p < 0.05$ *versus* erbB2 Ab; $n \geq 3$. Data are presented as mean ± S.E.

studies (Fig. 2, *A* and *B*). To determine whether treatment with erbB2-Ab increases ROS production, we treated cells with control IgG or erbB2-Ab then measured intracellular ROS production with fluorescent markers detected by flow cytometry and confocal microscopy. There was a statistically significant, dose-dependent increase in the amount of ROS produced with erbB2-Ab treatment (Fig. 2, *C* and *D*). To determine whether erbB2-Ab-associated cell death is a direct result of this increase in ROS, cells were treated with 1 μg/ml erbB2-Ab in the presence and absence of 10 mM NAC (a reducing agent and ROS scavenger). In cells treated with erbB2-Ab, NAC restored viability to the levels observed in control cells (Fig. 2E). These results suggest that treatment of NRCM with erbB2-Ab increases intracellular ROS levels, which results in cell death.

ErbB2 Signaling Occurs through a Mitochondrial Dependent Pathway—Because erbB2 blockade causes an increase in cellular ROS production, and the majority of ROS in the cell are produced in the mitochondria, we studied the role of mitochondria in erbB2 signaling. First, we determined the effects of erbB2-Ab on cyto *c* release into the cytoplasm. We treated NRCM with erbB2-Ab, and isolated protein from the mitochondrial and cytoplasmic fractions. Treatment of NRCM with erbB2-Ab resulted in a marked decrease in mitochondrial cyto *c* levels compared with IgG treatment (Fig. 3A).

To better characterize the link between the erbB2 pathway and mitochondria, we used cyclosporine A (CsA) to inhibit the mitochondrial permeability transition pore (mPTP), or diazoxide to activate the mitochondrial ATP-sensitive potassium channel (mitoK$_{ATP}$). Both CsA and diazoxide treatment reduced cell death caused by erbB2-Ab (Fig. 3B). Moreover, cells treated with CsA or diazoxide in combination with erbB2-Ab displayed significantly lower levels of ROS produc-
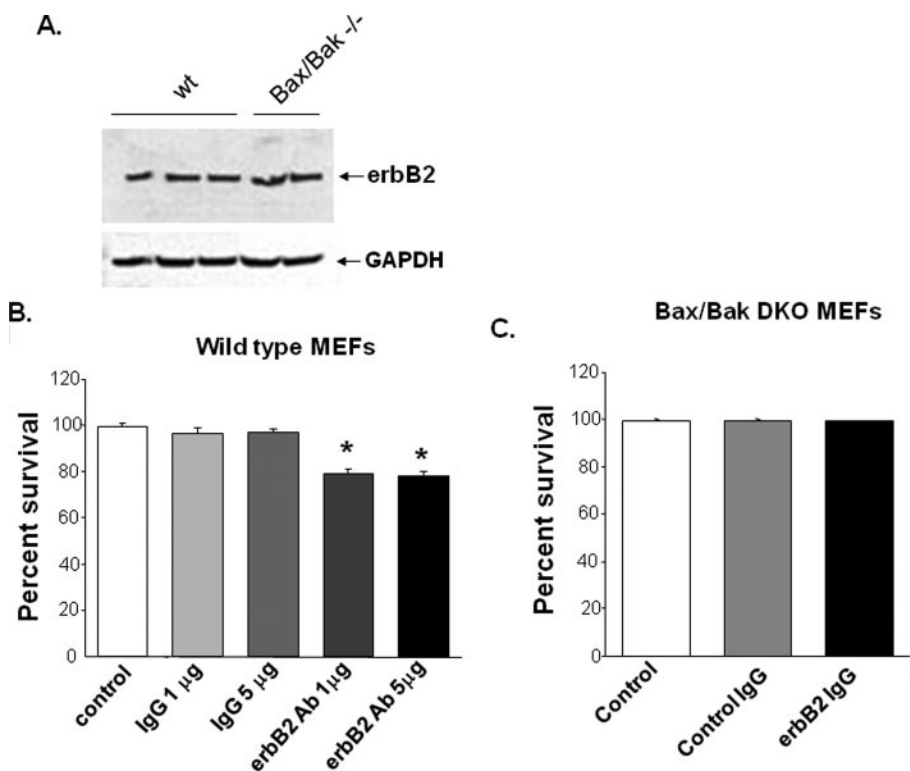
FIGURE 4. **erbB2 blockade requires Bax and Bak to induce cell death.** *A*, Western blot showing erbB2 expression in WT and Bax/Bak DKO MEFs. Quantification of trypan blue exclusion in (*B*) WT and (*C*) DKO MEFS after treatment with erbB2 Ab. *, $p = 6 \times 10^{-4}$ for 1 μg and $= 3 \times 10^{-4}$ for 5 μg of erbB2 Ab *versus* IgG; $n \geq 3$. Data are presented as mean $\pm$ S.E.
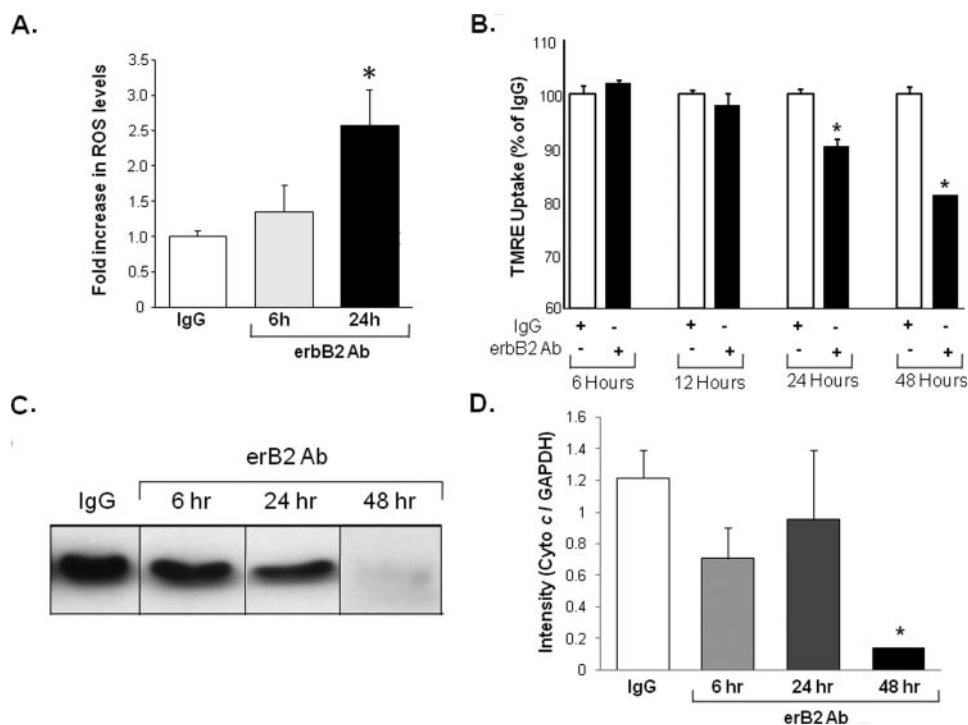

FIGURE 5. **ROS production precedes dissipation of the MMP and mitochondrial cyto *c* release.** *A*, the time course of ROS production in NRCM treated with erbB2 Ab or a control (IgG) Ab. Levels of ROS were measured with mitoSOX as described in Fig. 2. *B*, time course of TMRE uptake in NRCM treated with erbB2 Ab or a control (IgG) Ab. A partial reduction in TMRE uptake was observed 24 h after treatment, and uptake continued to decline at 48 h. *C*, Western blot of the mitochondrial fraction of NRCM treated with erbB2 Ab and probed with cyto *c* at different time points. *D*, quantification of cyto *c* levels in *C* (*, $p < 0.05$ *versus* control). Mitochondrial cyto *c* levels declined significantly 48 h after treatment. Band intensities were measured by using ImageJ and normalized to the internal control (actin). Data are presented as mean $\pm$ S.E.

tion than were measured in cells treated with erbB2-Ab alone (Fig. 3*C*). CsA also reduced baseline ROS, whereas diazoxide produced a significant effect only in the presence of erbB2. These results show that blocking the mPTP channel blocks the ROS-producing effects of erbB2-Ab treatment. This observation suggests that erbB2-Ab-induced ROS production and cell death occur through an mPTP-dependent pathway. Furthermore, activation of the pro-survival channel mitoK$_{ATP}$ can reverse this effect.

ErbB2-Ab-mediated Cell Death Is Regulated by a Bax/Bak-dependent Pathway—Growth factor-induced cell death is generally believed to be Bax/Bak-dependent (15). In response to an insult, these proteins translocate to the mitochondria and induce mitochondrial dependent cell death. To evaluate the role of Bax and Bak in erbB2-Ab-induced cell death, we examined cell death in WT mouse embryonic fibroblasts (MEFs) and in MEFs obtained from Bax/Bak double-knock-out (DKO) mice after treatment with erbB2-Ab or a control Ab. Wild type (WT) and DKO MEFs express similar levels of erbB2 at baseline (Fig. 4*A*). In WT MEFs, erbB2-Ab treatment significantly increased cell death compared with control-treated MEFs (Fig. 4*B*). However, in DKO MEFs, there was no increase in cell death associated with erbB2-Ab treatment (Fig. 4*C*). These results suggest that Bax and/or Bak are necessary for erbB2-Ab-mediated cell death, because their absence attenuated the cell death response associated with erbB2 blockade.

Time Course of the Deleterious Effects of erbB2-Ab—The data presented thus far suggest that blockade of the erbB2 receptor increases cell death through a mitochondrial and ROS-dependent pathway. These results raise the question of whether cyto *c* release into the cytoplasm precedes or follows mitochondrial changes and ROS production. To answer this question, we
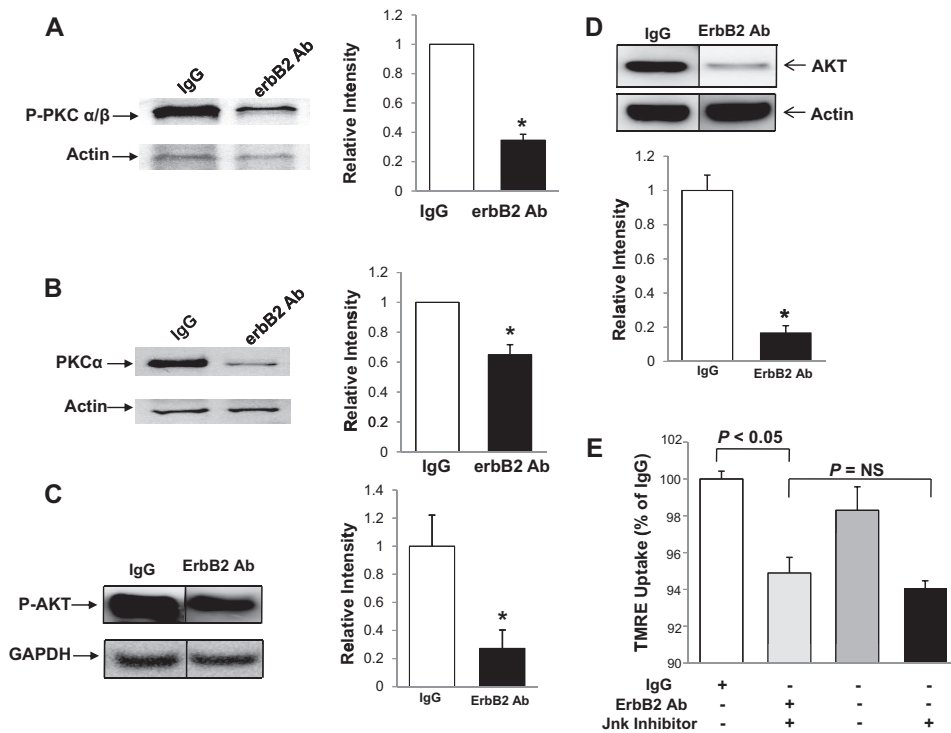
FIGURE 6. **erbB2 Ab-mediated signaling occurs through AKT- and PKCα-dependent pathways.** *A*, Western blot (*left*) and quantification (*right*, normalized to actin levels) of phosphorylated PKCα levels in NRCM treated with erbB2 Ab or a control (IgG) Ab and probed with an antibody against the phosphorylated form of PKCα *B*, Western blot (*left*) and quantification (*right*, normalized to actin levels) of PKCα levels in NRCM treated with erbB2 Ab or a control (IgG) Ab and probed with a PKCα antibody. *C*, Western blot (*left*) and quantification (*right*, normalized to GAPDH levels) of phosphorylated AKT levels in NRCM treated with erbB2 Ab or a control (IgG) Ab and probed with an antibody against phosphorylated AKT. *D*, Western blot (*top*) and quantification (*bottom*, normalized to actin levels) of AKT levels in NRCM treated with erbB2 Ab or a control (IgG) Ab and probed with an AKT antibody. *E,* flow cytometry analyses of TMRE uptake in NRCM treated with erbB2 Ab or a control (IgG) Ab in the presence and absence of JNK inhibitor IX. *, $p < 0.05$ *versus* control; #, $p < 0.05$ *versus* erbB2 Ab treated cells; $n = 3$ in each group. Data are presented as mean ± S.E.

analyzed the time course of ROS production, of changes in the mitochondrial membrane potential (MMP), and of the release of cyto *c* into the cytoplasm after treatment with erbB2-Ab or the control Ab. As shown in Fig. 5*A*, ROS production reaches significant levels 24 h after treatment, and the MMP (Fig. 5*B*) begins to change at 24 h and continues to decline at 48 h. However, the increase in cytoplasmic levels of cyto *c* does not reach statistical significance until about 48 h after treatment (Fig. 5, *C* and *D*). These results suggest that ROS production probably occurs before MMP loss and the release of cyto *c* into the cytoplasm, which subsequently results in cell death.

Effects of erbB2-Ab on Cardiomyocytes Occur through an AKT- and PKCα-dependent Pathway—We then studied the signaling mechanisms that lead to the deleterious effects of erbB2-Ab on cardiomyocytes. Previous reports suggested that PI3K and AKT have a role in erbB2-mediated signal transduction (16). It has also been shown that PKCα is up-regulated and activated in breast cancer in response to erbB2-receptor activation (17). Thus, we studied the role of PI3K, AKT, and PKCα in the erbB2-Ab-mediated pathway in the heart. NRCM were treated with the erbB2-Ab, and cell extracts were probed with AKT, p-AKT, and PKCα antibodies. Treatment with the erbB2-Ab resulted in a significant decrease in both total and phosphorylated AKT and PKCα protein (Fig. 6, *A–D*). These results suggest that the deleterious effects of erbB2-Ab are

likely mediated through the inhibition of AKT and PKCα signaling.

Reports also suggest that erbB2 signaling is mediated by a JNK-dependent pathway (18). To study the role of this protein in erbB2-Ab-mediated cardiomyocyte death, NRCM were treated with 10 μM JNK inhibitor IX (CalBiochem) in the presence of either IgG or erbB2-Ab. The JNK inhibitor did not significantly change the rate of cell death when cells were treated with IgG or erbB2-Ab (Fig. 6*E*). These results suggest that erbB2-Ab-mediated cell death in cardiomyocytes probably occurs independently of the JNK pathway.

Reduction of erbB2 Protein Increases Cell Death—To demonstrate that the effects of erbB2 blockade do not result from nonspecific Ab interactions, we used an siRNA that targets erbB2 as an alternative method for blocking erbB2 function. NRCM were treated with erbB2 or control siRNA for 48 h, and erbB2 protein levels were assessed by Western blotting. Treatment with the erbB2-specific siRNA significantly reduced erbB2 protein levels compared with control siRNA treatment (Fig. 7, *A* and *B*).

Next, we used this approach to study the effects of a reduction in erbB2 protein levels on cell survival. NRCM treated with erbB2 siRNA exhibited a significant increase in cell death as assessed via TMRE uptake and trypan blue exclusion assays (Fig. 7, *C* and *D*). These results are consistent with our findings that erbB2 blockade induces cell death and suggest that the effects of the erbB2-Ab likely result from the specific inhibition of the erbB2 pathway.

DISCUSSION

The cell surface tyrosine kinase receptor erbB2 plays an important role in a variety of cellular functions; however, it can also function as an oncogene in several malignancies, including breast, lung, and endometrial cancer (19, 20). Therefore, erbB2 has become an important target for breast cancer therapy. Data suggest that trastuzumab (Herceptin) improves survival in patients with metastatic disease, and when used as an adjuvant (4, 7); however, trastuzumab also contributes to the development of CM in a significant number of patients, especially in those who either have previously had anthracyclines or are treated with trastuzumab and anthracyclines together (8). ErbB2 has been shown to play a role in cardiac development, as cardiac-specific knock-out of this protein in mice leads to dilated CM. However, the mechanism of erbB2-Ab-mediated
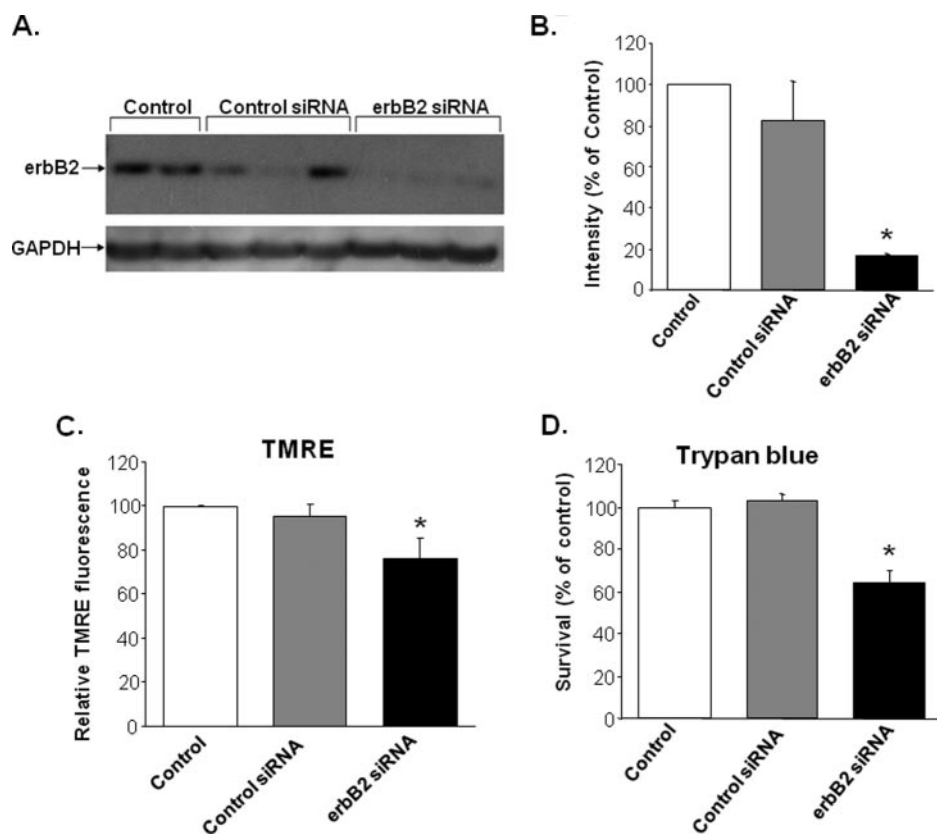
FIGURE 7. **Treatment of NRCM with erbB2 siRNA increases cell death.** *A*, Western blot of untreated (control) NRCM and NRCM treated with control siRNA or erbB2 siRNA. *B*, quantification of Western blot data from *A* normalized to GAPDH and expressed as a percentage of the control NRCM (*, $p = 2 \times 10^{-4}$ *versus* control siRNA; $n = 3$). *C*, flow cytometry analyses of TMRE uptake in untreated (control) NRCM and in NRCM treated with control siRNA or erbB2 siRNA (*, $p = 0.028$ *versus* control siRNA; $n \geq 3$). *D*, trypan blue exclusion assays of untreated (control) NRCM and NRCM treated with control siRNA or erbB2 siRNA (*, $p = 0.008$ *versus* control siRNA; $n \geq 3$). Data are presented as mean ± S.E.

cell death and the role of erbB2 in cell survival and in response to ischemic injury are not known.

In this study, we examined the mechanism of cell death induced by erbB2 inhibition. Because receptor-mediated cell death is believed to be regulated by mitochondria (15, 21, 22), we hypothesized that erbB2 blockade leads to activation of a mitochondrial pathway that results in an increase in cellular ROS production and subsequent cell death. To test this hypothesis, we treated NRCM with an inhibitory erbB2-Ab, then demonstrated that erbB2 blockade leads to an increase in ROS production, and that the deleterious effects of erbB2-Ab are reversed by the antioxidant NAC. We then showed that erbB2-Ab-mediated cell death is inhibited by an mPTP inhibitor and by an activator of mitoK$_{\text{ATP}}$, suggesting that mitochondria are involved in erbB2-Ab-mediated cell death. These chemicals also reversed erbB2-Ab-mediated ROS production. Finally, to demonstrate that the deleterious effects of erbB2-Ab on cardiomyocytes do not evolve from nonspecific effects of the Ab, we showed that erbB2 knockdown with siRNA increased cell death.

Our results are consistent with those of Grazette *et al.* (11) who showed that the erbB2-Ab mediates cell death. We also demonstrate that erbB2-Ab-mediated cell death signaling requires both Bax and Bak, as MEFs lacking these proteins were resistant to the deleterious effects of erbB2-Ab. These data are

in accord with the generally accepted model that receptor-mediated cell death occurs through a mitochondrial and Bax/Bak-dependent pathway (15).

Our findings not only provide mechanistic insights into the biological effects of erbB2-receptor blockade, they may also have therapeutic implications. Patients with breast cancer who receive trastuzumab may develop heart failure. Because our understanding of how erbB2 signaling leads to myocardial cell death is limited, there are no effective approaches to attenuate the deleterious effects of trastuzumab on the heart. Our current results provide evidence for two potential therapeutic targets for the prevention of trastuzumab-induced CM: cellular ROS and mitochondria. Cellular ROS are significantly increased after treatment with erbB2-Ab; however, an antioxidant may reverse this effect. Thus, concurrent antioxidant therapy with trastuzumab may attenuate the adverse effects of this drug on the heart. Furthermore, our results provide evidence that erbB2-Ab-induced cell death occurs through a mitochondrial pathway. Therefore,

patients who receive trastuzumab may also benefit from drugs that inhibit mPTP or activate the protective mitoK$_{\text{ATP}}$ channel. The effectiveness of these interventions requires further study.

The levels of many proteins are altered in response to ischemic injury in the heart. Here, we show that erbB2 levels decrease in response to both acute ischemia and chronic ischemic damage. The observation that patients with chronic ischemic CM displayed lower levels of erbB2 suggests that erbB2 may be an important factor in ischemic damage of the heart. These results, along with our observation that diminished erbB2 signaling results in an increase in cell death, suggest that erbB2 is important for normal cardiomyocyte function. Furthermore, changes in the activity of erbB2 may make heart cells more susceptible to injury from ischemic damage. Thus, increasing the activity of erbB2 in the ischemic heart may prove to be a novel therapeutic tool for treating ischemic heart disease.

In summary, our results indicate that erbB2 blockade leads to cell death through mitochondrial and ROS-dependent pathways. We also show that erbB2-mediated cell death occurs through AKT- and PKCα-dependent pathways. Furthermore, both acute and chronic ischemic damage to the heart decreased erbB2 levels. These findings suggest that concomitant therapy with agents that regulate redox signaling (such as antioxidants)

or target mitochondrial death channels may reduce cardiac injury from trastuzumab in cancer patients.

REFERENCES

1. Groenen, L. C., Nice, E. C., and Burgess, A. W. (1994) *Growth Factors* **11,** 235–257
2. Lemke, G. (1996) *Mol. Cell Neurosci.* **7,** 247–262
3. Slamon, D. J., Clark, G. M., Wong, S. G., Levin, W. J., Ullrich, A., and McGuire, W. L. (1987) *Science* **235,** 177–182
4. Slamon, D. J., Godolphin, W., Jones, L. A., Holt, J. A., Wong, S. G., Keith, D. E., Levin, W. J., Stuart, S. G., Udove, J., and Ullrich, A. (1989) *Science* **244,** 707–712
5. Toikkanen, S., Helin, H., Isola, J., and Joensuu, H. (1992) *J. Clin. Oncol.* **10,** 1044–1048
6. Di Carlo, E., Diodoro, M. G., Boggio, K., Modesti, A., Modesti, M., Nanni, P., Forni, G., and Musiani, P. (1999) *Lab. Investig.* **79,** 1261–1269
7. Slamon, D. J., Leyland-Jones, B., Shak, S., Fuchs, H., Paton, V., Bajamonde, A., Fleming, T., Eiermann, W., Wolter, J., Pegram, M., Baselga, J., and Norton, L. (2001) *N. Engl. J. Med.* **344,** 783–792
8. Keefe, D. L. (2002) *Cancer* **95,** 1592–1600
9. Crone, S. A., Zhao, Y. Y., Fan, L., Gu, Y., Minamisawa, S., Liu, Y., Peterson, K. L., Chen, J., Kahn, R., Condorelli, G., Ross, J., Jr., Chien, K. R., and Lee, K. F. (2002) *Nat. Med.* **8,** 459–465
10. Ozcelik, C., Erdmann, B., Pilz, B., Wettschureck, N., Britsch, S., Hubner, N., Chien, K. R., Birchmeier, C., and Garratt, A. N. (2002) *Proc. Natl. Acad. Sci. U. S. A.* **99,** 8880–8885
11. Grazette, L. P., Boecker, W., Matsui, T., Semigran, M., Force, T. L., Hajjar, R. J., and Rosenzweig, A. (2004) *J. Am. Coll Cardiol.* **44,** 2231–2238
12. Timolati, F., Ott, D., Pentassuglia, L., Giraud, M. N., Perriard, J. C., Suter, T. M., and Zuppinger, C. (2006) *J. Mol. Cell Cardiol.* **41,** 845–854
13. Decker, R. S., Decker, M. L., Kulikovskaya, I., Nakamura, S., Lee, D. C., Harris, K., Klocke, F. J., and Winegrad, S. (2005) *Circulation* **111,** 906–912
14. Ardehali, H., O'Rourke, B., and Marban, E. (2005) *Circ. Res.* **97,** 740–742
15. Wei, M. C., Zong, W. X., Cheng, E. H., Lindsten, T., Panoutsakopoulou, V., Ross, A. J., Roth, K. A., MacGregor, G. R., Thompson, C. B., and Korsmeyer, S. J. (2001) *Science* **292,** 727–730
16. Fuller, S. J., Sivarajah, K., and Sugden, P. H. (2008) *J. Mol. Cell Cardiol.* **44,** 831–854
17. Tan, M., Li, P., Sun, M., Yin, G., and Yu, D. (2006) *Oncogene* **25,** 3286–3295
18. Le, X. F., Arachchige-Don, A. S., Mao, W., Horne, M. C., and Bast, R. C., Jr. (2007) *Mol. Cancer Ther.* **6,** 2843–2857
19. Roskoski, R., Jr. (2004) *Biochem. Biophys. Res. Commun.* **319,** 1–11
20. Schlessinger, J. (2000) *Cell* **103,** 211–225
21. Luo, X., Budihardjo, I., Zou, H., Slaughter, C., and Wang, X. (1998) *Cell* **94,** 481–490
22. Li, H., Zhu, H., Xu, C. J., and Yuan, J. (1998) *Cell* **94,** 491–501